International Journal of Smart Home
Vol. 10, No. 4 (2016), pp. 129-142
http://dx.doi.org/10.14257/ijsh.2016.10.4.13

Threshold Selection for 60 GHz TOA Estimation Based on Skewness and Kurtosis Analysis

Xiao-Lin Liang[1], Hao Zhang[1, 2], Ting-Ting Lu[1] and T. Aaron. Gulliver[2]

[1]College of Information Science and Engineering, Ocean University of China, Qingdao, 266100, China;
[2]Department of Electrical and Computer Engineering, University of Victoria, Victoria V8W 3P6, Canada
xiaolin87liang@163.com, zhanghao@ouc.edu.cn
lvtingting33@163.com, agullive@ece.uvic.ca

Abstract

Because of the high sampling rate, coherent Time of Arrival (TOA) estimation algorithms are not practical for low cost, low complexity 60 GHz systems. In this paper, energy detect (ED) based non-coherent TOA estimation algorithm is presented. The expected values of the skewness and kurtosis with respect to the signal to noise ratio (SNR) are investigated. It is shown that the ratio of kurtosis and skewness is more suitable for TOA estimation. To improve the precision of TOA estimation, a new threshold selection algorithm is proposed which is based on the ratio of kurtosis and skewness analysis. The best threshold values for different SNRs are investigated and the effects of integration period and channel modes are examined. Comparisons with other ED based algorithms show that in CM1.1 and CM2.1 channels, the proposed algorithm provides higher precision and robustness in both high and low SNR environments.

***Keywords**: 60 GHz, ED, TOA estimation, skewness, kurtosis*

1. Introduction

The demand for high data rate wireless communications with low latency has increased dramatically in recent years. Unfortunately, due to spectrum limitations and transmit power regulations, current short-range wireless communication strategies cannot achieve Gigabit per second (Gbps) data rates. Fortunately, wireless communications in the 60 GHz millimeter wave (mm-wave) band has become viable for Gbps wireless communication networks [1-4] due to the availability of several GHz of license-free spectrum, up to 10 W maximum transmit power, no interference from other systems, and the development of low-cost complementary metal-oxide semiconductor (CMOS) devices. The Federal Communications Commission (FCC) permits communications in the 60 GHz unlicensed band at an effective isotropic radiated power (EIRP) of up to 40 dBm, which is many times greater than other short-range wireless communication strategies. In China, this limit is 44 dBm [5]. Although the path loss (PL) is high at 60 GHz, the received power can still be significant. IR communication strategies have been proposed for this frequency band because it can be effective in separating the multipath signals at the receiver. This is because short pulses are employed for communications with a duration (typically under 100 picoseconds), which is far less than the multipath propagation delay. These signals can also provide the fine multipath resolution required for high precision ranging and localization [6]. Thus, the 60 GHz signals are even much suitable for localization applications for short distances.

Generally, the localization strategies can be classified into time based [7-10] and non-time based [11]. For example, TOA [10-12] and Time Difference of Arrival (TDOA)

ISSN: 1975-4094 IJSH

[10] are time based strategies, while Received Signal Strength (RSS) and Angle of Arrival (AOA) [11] are non-time based. Localization that based on time (TOA or TDOA) is even much suitable for using with 60 GHz strategy [11], as it can take full advantage of the higher time and multipath resolution available with very short 60 GHz signals. TOA estimation which is even much more accurate is the key to accurate ranging, but this is very challenging due to the potentially hundreds of multipath components in 60 GHz channels, even in the non-line of sight (NLOS) environments. TOA estimation has been extensively studied [12, 15-18] for the past few years. There are two approaches which are much more applicable for TOA estimation, a Matched Filter (MF) [16] (such as a rake or correlation receiver) with a higher sampling rate and higher precision correlation, or an ED [18] with a lower sampling rate and lower complex. An MF is the optimal strategy for TOA estimation, where a correlator template is matched exactly to the received signal. However, a receiver operating at the Nyquist sampling rate makes it very difficult to align with the multipath components of the received signal [15]. In addition, an MF requires a priori estimation of the channel, including the timing, fading coefficient, and pulse shape for each component of the impulse response [15]. Because of the higher sampling rates and channel estimation, an MF may not be practical in many applications. As opposed to a more complex MF, an ED is a non-coherent approach to TOA estimation. It consists of a square-law device, followed by an integrator, sampler and a decision mechanism. The TOA estimate is made by comparing the integrator output with a threshold and choosing the first sample to exceed the threshold. This is a convenient strategy that directly yields an estimate of the start of the received signal. Thus, a low complexity, low sampling rate receiver can be employed without the need for a priori channel estimation.

The major challenge with ED is the selection of an appropriate threshold based on the received signal samples. In [17], a normalized threshold selection strategy for TOA estimation was proposed which exploits the Kurtosis of the received samples. In [18], an approach based on the minimum and maximum sample energy was introduced. Threshold selection for different SNR values was investigated via simulation. These approaches have limited TOA precision, as the strongest path is not necessarily the first arriving path.

In this paper, we consider the relationship between the SNR and the statistics of the integrator output including kurtosis and skewness. A metric based on the ratio kurtosis and skewness is then developed for threshold selection. The threshold for different SNR values is investigated and the effects of the integration period and channel are examined. Performance results are presented which show that in both the CM1.1 and CM2.1 channels, this joint metric provides higher precision and robustness.

The remainder of this paper is organized as follows. In Section 2, the system model is outlined. Section 3 discusses various TOA estimation algorithms based on ED. Section 4 considers the statistical characteristics of the energy values. In Section 5, a joint metric based on the ratio of kurtosis and skewness is proposed, a novel TOA estimation algorithm is introduced. Some performance results are presented in Section 6 and Section 7 concludes the paper.

2. System Model

Currently, there are two important standards that have been developed for the 60 GHz wireless communications systems, IEEE 802.15.3c and IEEE 802.11ad [19-20]. In this paper, the channel models in IEEE 802.15. 3c standard are used because it is specifically designed for Wireless Personal Area Networks (WPAN) and thus encompasses typical indoor environments. Further, these are the most widely employed models for the 60 GHz systems. The IEEE 802.15.3c standard was the first developed for high data rate short-range wireless systems. The physical layer was designed to support the transmission of data within a few meters at a minimum data rate of 2 Gbps. These models have been developed for communications in the frequency band 57 to 66 GHz in indoor residential, indoor office and library environments (with differences largely due to the LOS and NLOS characteristics) [21-25].

In this paper, a Pulse Position Modulation Time Hopping (PPM-TH) 60 GHz signal is employed for ranging purposes. The propagation delay $\hat{\tau}$, between the transmitter and receiver is estimated for use in localization.

2.1. 60 GHz Signal

The 2PPM-TH-60 GHz signals have a very short duration (typically 100 picoseconds or less), and can be expressed as:

$$s(t)=\sum_{-\infty}^{\infty} p\left(t-jT_s-C_jT_c-a_j\varepsilon\right) \quad (1)$$

Each symbol is represented by a sequence of very short pulses.
where T_s is the symbol time. The Time Hopping (TH) code represented by *Cj* is a pseudorandom integer-valued sequence which is unique for each user to limit multiple access interference, and T_c is the chip time. The PPM time shift is ε so that if a_j is 1, the signal is shifted in time by ε, while a_j is 0, there is no shift. In general, these parameters satisfy the following relationship:

$$(1)\, C_jT_c+\varepsilon<T_s;$$
$$(2)\, \varepsilon<T_c;$$
$$(3)\, a_j\varepsilon<C_jT_c\left(C_j\neq 0\right)$$

Many pulse shapes have been proposed for 60 GHz systems. In this paper a Gaussian pulse is employed which is multiplied by the carrier signal to give as shown in the Figure1 [26]

$$p(t)=\frac{\sqrt{2}}{\alpha}\exp\left(-2\pi\frac{t^2}{\alpha^2}\right)\cos\left(2\pi f_c t\right) \quad (2)$$

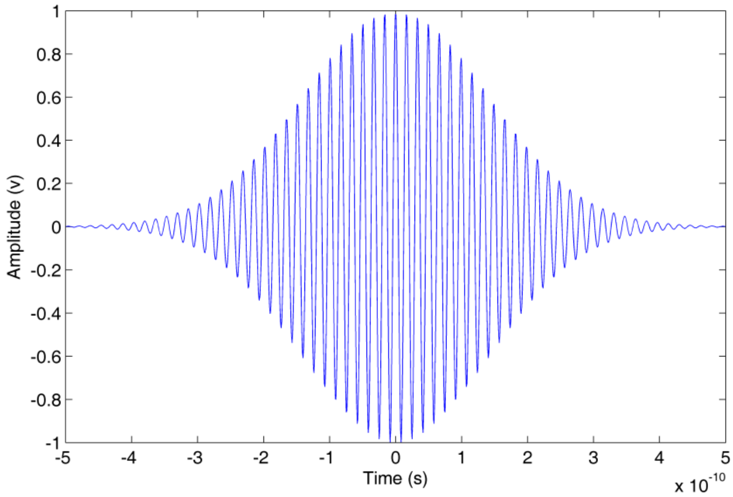

Figure 1. Waveform of the 60 GHz Signal

where α is the shape factor, and f_c is the carrier frequency which here is $f_c=60$ GHz. A smaller shape factor results in a shorter duration pulse and a larger bandwidth.

2.2. Multipath Fading Channel

The received signal can be written as:

$$r(t)=\sum_{n=1}^{N}\alpha_n p(t-\tau_n)+n(t) \tag{3}$$

where N is the number of received multipath components, α_n and τ_n denotes the amplitude and delay of the *nth* path respectively, $p(t)$ is the received 60 GHz pulse and $n(t)$ is Additive White Gaussian Noise (AWGN) with zero mean and two sided power spectral density $N_0/2$. Equation (3) can be rewritten as:

$$r(t)=s(t)*h(t)+n(t) \tag{4}$$

where $s(t)$ is the transmitted signal, and $h(t)$ is the channel impulse response which can be expressed as:

$$h(t,\theta)=\sum_{k=1}^{K}\sum_{l=1}^{L_k}\mu_{kl}\delta(t-T_k-\tau_{kl})\delta(\theta-\theta_k-\omega_{kl}) \tag{5}$$

where $\delta(.)$ is the dirac-delta function, K is the number of clusters, L_k is the number of rays in the k^{th} cluster, and μ_{kl} , τ_{kl} and ω_{kl} denote the complex amplitude, delay and azimuth of the k^{th} ray of the l^{th} cluster, respectively. Similarly, T_k and θ_k represent the delay and mean angle of arrival of the k^{th} cluster.

2.3. Energy Detector

As shown in Figure 2 [27], after the amplifier, the received signals are squared, and then input to an integrator with integration period Tb . Because of the inter-frame leakage due to multipath signals, the integration duration is $3T_f/2$, so the number of signal values for ED is $N=3T_f/2Tb$. The integrator outputs can be expressed as:

$$z[n]=\sum_{i=1}^{N}\int_{(i-1)T_f+(c_j+n-1)Tb}^{(i-1)T_f+(c_j+n)Tb} r^2(t)dt \tag{6}$$

where $n\in\{1,2,..,N\}$ denotes the sample index with respect to the starting point of the integration period and N is the number of pulses per symbol. Here, N is set to 1, so the integrator outputs are

$$z[n]=\sum_{i=1}^{N}\int_{(c_j+n-1)Tb}^{(c_j+n)Tb} r^2(t)dt \tag{7}$$

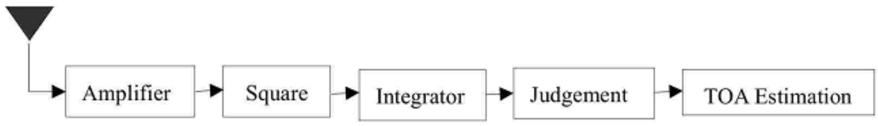

Figure 2. Block Diagram of the Energy Detector Receiver

If $z[n]$ is the integration of noise only, it has a centralized Chi-square distribution, while it has a non-centralized Chi-square distribution if a signal is present. The mean and variance of the noise and signal values are given by [17] respectively.

$$\mu_0=F\sigma^2,\sigma_0=2F\sigma^4 \tag{8}$$

$$\mu_e = F\sigma^2 + E_n, \sigma_e^2 = 2F\sigma^4 + 4\sigma^2 E_n \tag{9}$$

where E_n is the signal energy within the nth integration period and F is the number of degrees of freedom given by $F = 2BTb+1$. Here B is the signal bandwidth.

3. TOA Estimation Based on ED

3.1. TOA Estimation Algorithms

There are many TOA estimation algorithms based on ED for determining the start block of a received signal. The simplest is Maximum Energy Selection (MES), which chooses the maximum energy value to be the start of the signal value. The TOA is estimated as the center of the corresponding integration period:

$$\tau_{MES} = \left[\underset{1 \le n \le N_b}{\arg\max} \{z[n]\} - 0.5 \right] Tb \tag{10}$$

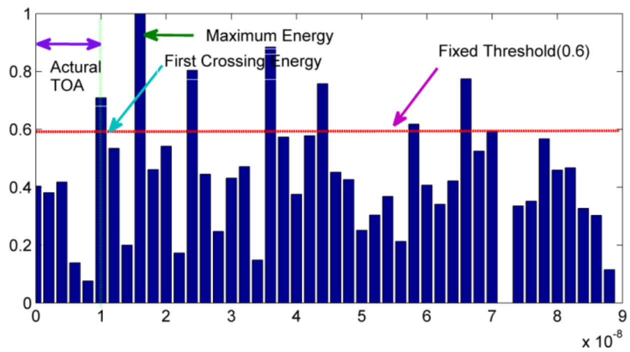

Figure 3. TOA Estimation Based on Energy Detector

However, as show in Figure 3, the maximum energy value may not be the first energy block [13], especially in NLOS environments. On average, the first energy value $z[n]$ is located before the maximum $z[n_{\max}]$, i.e. $n \le n_{\max}$. Thus, Threshold Crossing TOA estimation has been proposed where the received energy values are compared to an appropriate threshold α. In this case, the TOA estimation is given by:

$$\tau_{TC} = \left\{ \left(\underset{1 \le n \le n_{\max}}{\arg\min} \left[n \mid z(n) \ge \alpha \right] \right) - 0.5 \right\} Tb \tag{11}$$

It is difficult to determine an appropriate threshold α directly, so usually a normalized threshold α_{norm} is calculated. Using α_{norm}, α is given by:

$$\alpha = \alpha_{norm} \left\{ \max\left[z(n)\right] - \min\left[z(n)\right] \right\} + \min\left[z(n)\right] \tag{12}$$

The TOA (τ_{TC}) is then obtained using (11). A simpler threshold crossing algorithm is the Fixed Threshold algorithm where the threshold is set to a fixed value, for example α_{norm} =0.4 .The problem in this case becomes one of how to set the threshold. It should be based on the statistics of the signal energy, particularly for multipath, NLOS indoor environments.

3.2. Error Analysis

The Mean Absolute Error (MAE) of TOA estimation based on threshold crossing was analyzed, and closed form error expressions derived. The MAE can be used to evaluate the quality of an algorithm, and is defined as:

$$MAE = \frac{1}{N}\sum_{n=1}^{N}\left(t_n - t_n\right) \qquad (13)$$

where t_n is the *nth* actual propagation time, t_n is the *nth* TOA estimate, and *N* is the number of TOA estimates.

4. Statistical Characteristics

In this section, the kurtosis and skewness of the energy blocks are analyzed.

4.1. Kurtosis

The kurtosis is calculated using the second and fourth order moments and is given by:

$$k = \frac{E\left[\left(x_i - \mu_x\right)^4\right]}{E\left[\left(x_i - \mu_x\right)^2\right]^2} = \frac{E\left[\left(x_i - \mu_x\right)^4\right]}{\sigma_x^4} \qquad (14)$$

where μ_x is the mean value, and σ_x is the. The kurtosis for a standard normal distribution is three. For this reason, kurtosis is often redefined as $K = K - 3$ (often referred to as "excess kurtosis"), so that the standard normal distribution has a kurtosis of zero, positive kurtosis indicates a "peaked" distribution and negative kurtosis indicates a "flat" distribution.

For noise only (or for a low SNR) and sufficiently large *F* (degrees of freedom of the Chi-square distribution), $z[n]$ has a Gaussian distribution and kurtosis=0. On the other hand, as the SNR increases, kurtosis will tend to increase.

4.2. Skewness

The skewness is given by:

$$S = \frac{1}{\left(N-1\right)\delta^3}\sum_{i=1}^{N}\left(x_i - \mu_x\right)^3 \qquad (15)$$

where μ_x is the mean value, and δ is the standard deviation of the energy values. The skewness for a normal distribution is 0; in fact any symmetric data will have a skewness of zero. Negative values of skewness indicate that the data is skewed left, while positive values indicate data that is skewed right. Skewed left indicates that the left tail is long relative to the right tail, while skewed right indicates the opposite.

For noise only (or very low SNR) and sufficiently large *F*, skewness will tend to be 0. As the SNR increases, skewness will tend to increase.

4.3. Characteristics of the Parameters

In order to examine the characteristics of the three parameters (kurtosis and skewness), the CM1.1 (residential LOS) and CM2.1 (residential NLOS) channel models from the IEEE802.15.3c standard are employed. For each SNR value, 1000 channel realizations are generated and sampled at $f_c = 1 \cdot e^{10}$ Hz. The other system parameters are $T_f = 200ns$, $T_c = 1ns$, *Tb* = 1ns and 4ns and *N* = 1. Each realization has a TOA uniformly distributed within $\left(0 - T_f\right)$.

The two statistical parameters were calculated, and the results obtained are shown in Figure 3. This shows that the characteristics of the parameters with respect to the SNR are similar for the two channels. Further, Figure 3 shows that the ratio of kurtosis and skewness, kurtosis and skewness increase as the SNR increases, but the ratio changes more rapidly. Since the ratio changes more rapidly than the skewness and kurtosis, it better reflects changes in SNR, and so is more suitable for TOA estimation. Based on the results, a joint metric for TOA estimation is formulated as:

$$G = K / S \tag{16}$$

where S is the Skewness and K is the kurtosis.

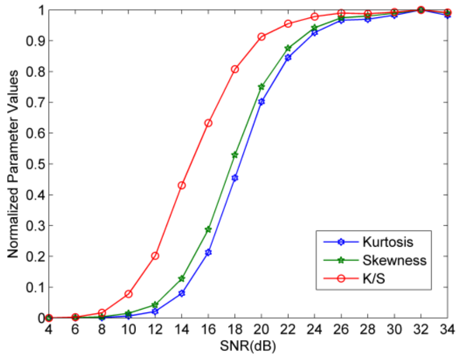

(1)CM1.1 and Tb=1ns

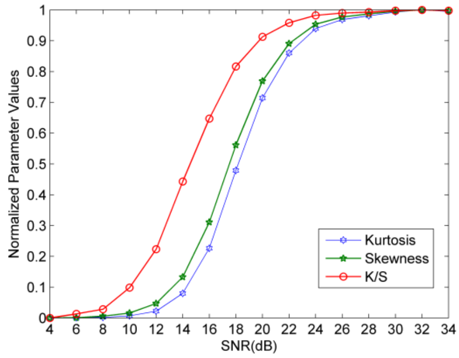

(2)CM1.1 and Tb=4ns

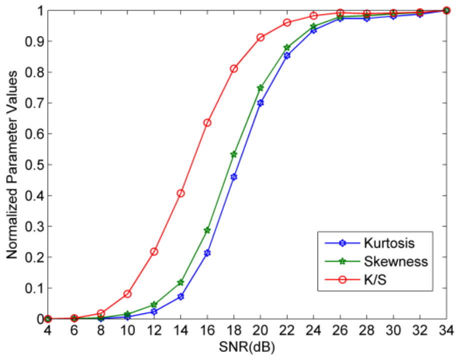

(3)CM2.1 and Tb=1ns

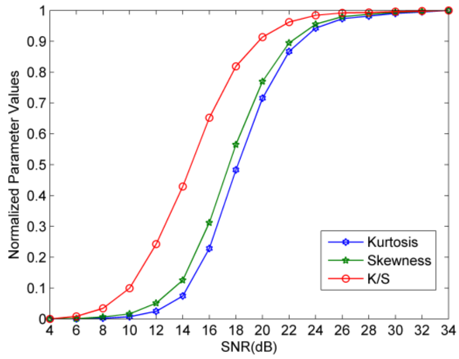

(4)CM2.1 and Tb=4ns

Figure 3. Parameters Change with SNR

5. Optimal Threshold Selection

5.1. Relationship between MAE and Normalized Threshold

In order to determine the best threshold (α_{best}) based on G, the relationship between MAE and normalized threshold (α_{norm}) was investigated. 1000 channel realizations with SNR = {4, 5,…, 34} dB were simulated under CM1.1 and CM2.1 environments. α is the threshold which is compared to the energy values to find the first threshold crossing. When α is bigger than $z[n_{\max}]$, we can't get the TOA estimation, so in this case, α is set to be 1.

In the simulation, all G values were rounded to the nearest integer and half-integer values for all SNR values. Figure 4 show the relationship between MAE and the normalized threshold in the CM1.1 and CM2.1 channels, respectively with Tb = 1ns and 4ns. The relationship is always that the MAE decreases as G increases. Another conclusion is that the minimum MAE is lower as G increases. The normalized threshold α_{norm} with respect to the minimum MAE is just the best threshold α_{best} . The relationship between α_{best} and G will be shown in the next section.

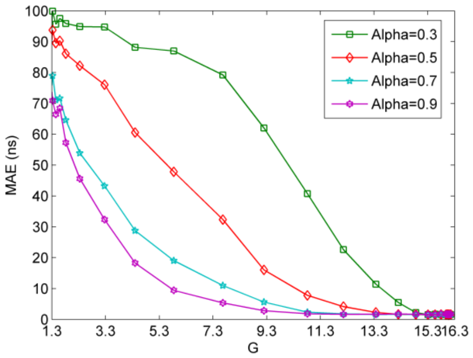

(1)CM1.1 and Tb=1ns

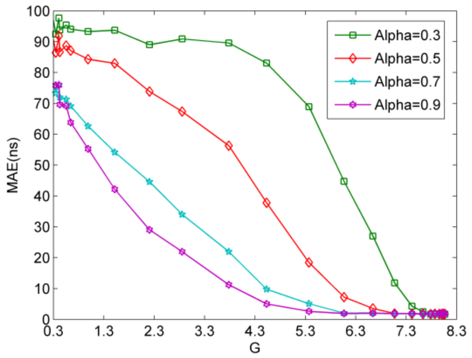

(2)CM1.1 and Tb=4ns

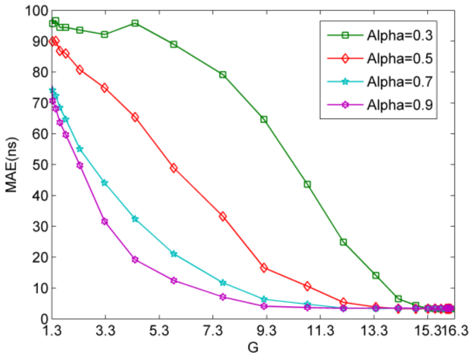

(3)CM2.1 and Tb=1ns

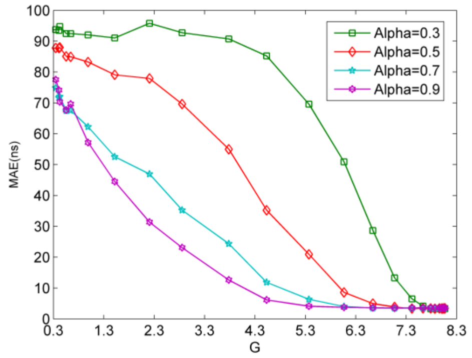

(4)CM2.1 and Tb=4ns

Figure 4. MAE with Respect to G

5.2. Optimal Thresholds

The normalized threshold α_{norm} with respect to the minimum MAE is called the best threshold α_{best} for a given G. Therefore, the lowest points of the curves in Figure 4 for each G are selected as the α_{best} .

As shown in Figure 5, these results show that the relationship between the two parameters is not affected significantly by the channel model, but is more dependent on the integration period, so the values for channels CM1.1 and CM2.1 can be combined. Therefore, the average of the two values is used as the optimal normalized threshold, as shown in (17).

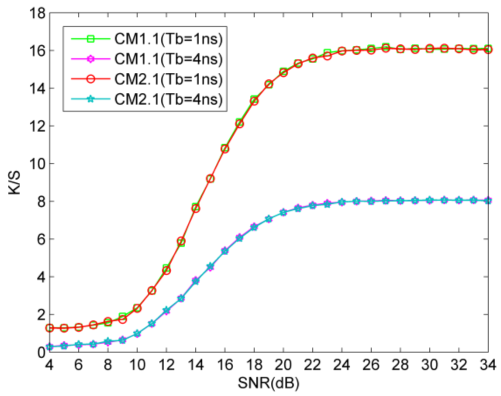

Figure 5. K/S with Respect to SNR

$$\alpha_{opt}^{(Tb)}(G)=\frac{\alpha_{best}^{(CM1.1,Tb)}(G)+\alpha_{best}^{(CM2.1,Tb)}(G)}{2} \tag{17}$$

Here two functions were fitted to these results for Tb = 4ns and 1ns, with G as the x-coordinate and α_{best} as the y-coordinate. An exponential function was used, giving

$$\alpha_{best}(1ns)=\begin{cases}0.8 & x<3.3\\ 7.49e^{-6}x^5-3.887e^{-4}x^4+6.575e^{-3}x^3-0.0483x^2+0.1582x+ & \\ 0.7116 & 3.3\le x<16.3\\ 0.1 & 16.3\le x\end{cases} \tag{18}$$

$$\alpha_{best}(4ns)=\begin{cases}0.8 & x<1.5\\ -1.952e^{-3}x^4+0.02852x^3-0.1564x^2+0.3859x+ & \\ 0.54 & 1.5\le x<8\\ 0.1 & 8\le x\end{cases} \tag{19}$$

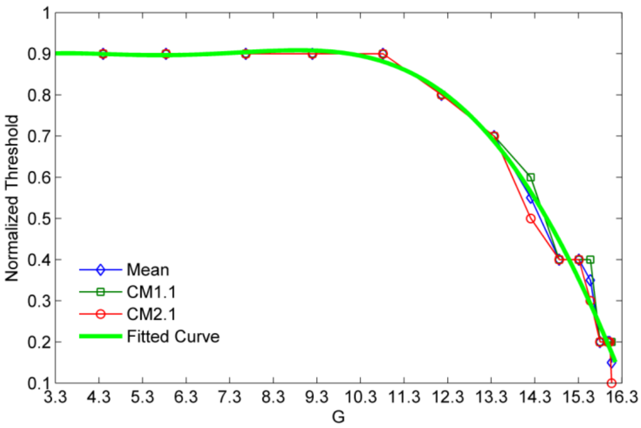

Figure 6. Normalized Threshold with Respect to *G* (*Tb* = 1ns)

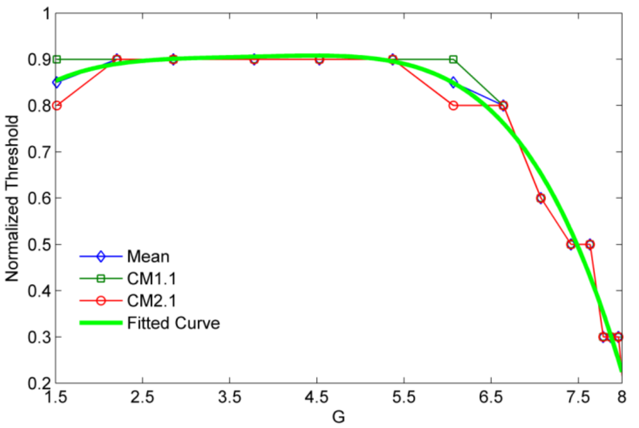

Figure 7. Normalized Threshold with Respect to *G* (*Tb* = 4ns)

6. Results and Discussion

In this section, the MAE is examined for different TOA estimation algorithms which based on Energy Detecting in the IEEE 802.15.3c CM1.1 and CM2.1 channels. 1000 channel realizations are generated and other parameters are set to be as above.

The MAE for SNR values from 4 dB to 34 dB in LOS (CM1.1) is presented in the Figure 8, the MAE for SNR values from 4 dB to 34 dB in NLOS (CM2.1) is presented in the Figure 9. This shows that the proposed algorithm performs even much better than other algorithm such as MES and fixed threshold. The performance in CM1.1 is better than in CM2.1 aiming at the same *Tb*. In most cases, the performance with *Tb* = 1ns is better than *Tb* = 4ns that with regardless of the channel. The MAE performance with three TOA algorithms in channels CM1.1 and CM2.1 are shown in Figures 8-9 respectively. Here “MES” is the Maximum Energy Selection algorithm, and the normalized threshold for the Fixed Threshold algorithm is set to 0.4 and 0.6. The MAE with the proposed algorithm is lower than other algorithms, particularly at low to moderate SNR values. The proposed algorithm is better except when the SNR is greater than 20 dB. The performance of the proposed algorithm is more robust than the other algorithms, as the performance difference is very small compared to the difference with other algorithms. For almost all SNR values the proposed algorithm is even much better. Conversely, the performance of other algorithms varies greatly and is very bad for low to moderate SNR values.

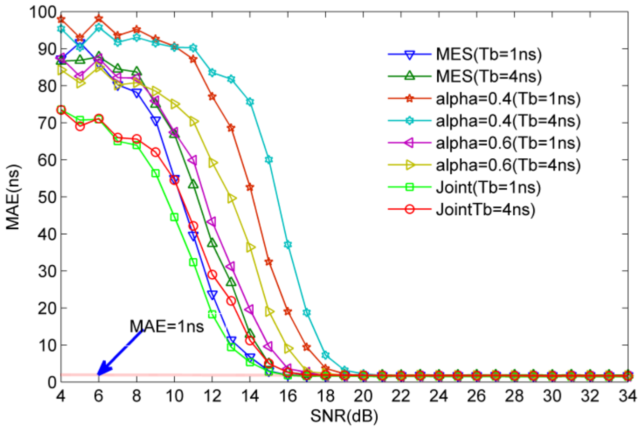

Figure 8. MAE for Different Algorithms with CM1.1

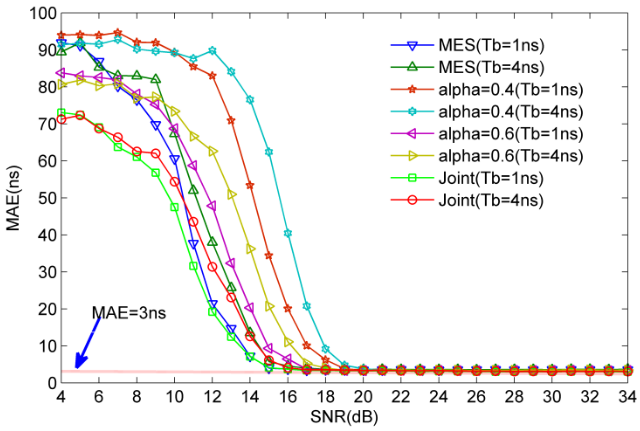

Figure 9. MAE for Different Algorithms with CM2.1

7. Conclusion

Low complexity, energy-based TOA estimation algorithms have been examined for 60 GHz ranging, positioning, and tracking applications. Two statistical parameters were investigated, and based on the results-obtained, a new algorithm based on the ratio kurtosis and skewness was developed for Threshold-Crossing TOA estimation. The best normalized threshold was determined using simulation with the CM1.1 and CM2.1 channels and curve fitting. The effects of the integration period and channel model were investigated. It was determined that the proposed threshold selection technique is largely independent of the channel model. The performance of the proposed algorithm was shown to be better than several known algorithms. In addition, the proposed algorithm is more robust to changes in the SNR and integration period.

Acknowledgments

The authors would like to thank colleagues from the UWB Laboratory in the College of Information Science and Engineering, Ocean University of China, for help with obtaining the measurement data. This work was supported by the Nature Science Foundation of China under Grant No. 60902005, the Qingdao International Science and Technology Cooperation Projects of Qingdao under Grant No. 12-1-4-137-hz, the Nature Science Foundation of China under Grant No. 61301139, the Nature Science Foundation of Shandong Province No. ZR2014FL014, the Science and Technology Project in Colleges and Universities of Shandong Province No.J14LN53, the Project of Basic Research Application of Qingdao City No. 14-2-4-37-jch and the Project of Basic Research Application of Qingdao City No. 14-2-4-83-jch.

References

[1] L. Zhang, "A fully integrated 60GHz five channel CMOS receiver with 7GHz ultra-wide band width for IEEE 802.11ad standard", Communication, China, vol. 11, no. 6, **(2014)**, pp. 42-50.
[2] S. K. Yong and C. C. Chong, "An overview of multi gigabit wireless through millimeter Wave Strategy: Potentials and Technical Challenges", EURASIP J. Wireless Communications and Networking, vol. 2007, no. 1, **(2007)**, pp. 1-10.
[3] R. C. Daniels and R. W. Heath, "60 GHz wireless communications: emerging requirements and design recommendations", IEEE Vehicular Strategy Society, vol. 2, **(2007)**, pp. 41-50.
[4] C. C. Chong, F. M. Peter, Smulders, "60GHz-Millimeter-Wave Radio Principle, Strategy, and News Results", EURASIP Journal on Wireless Communications and Networking, vol. 2007, no. 1, **(2007)**, pp. 1-8.
[5] S. K. Yong, P. F. Xia P F and Alberto V G, "60-GHz Strategy for Gbps WLAN and WPAN: From Theory to Practice", Beijing: Press of China Machine, **(2013)**.
[6] R. C. Daniels and R. W. Health, "60 GHz wireless communications: emerging requirements and design recommendations", IEEE Vehicular Strategy Magazine, vol. 2, no. 3, **(2007)**, pp. 41-50.
[7] D. Jie, X. Cui, H. Zhang and G. Wang, "A ultra-wideband location algorithm based on neural network". International Conference on Wireless Communications Networking and Mobile Computing (WiCOM), vol. 11, no. 6, (**2010)**, pp. 56-64.
[8] X. Tu, H. Zhang, X. Cui and T. A. Gulliver, "3D TDOA/AOA location based on extended Kalman filter", International Symposium on Antennas, Propagation and EM Theory (ISAPE), vol. 11, no. 6, (**2010)**, pp. 56-64.
[9] Z. Sahinoglu and S. Gezici, "Ranging in the IEEE 802.15.4a standard", in IEEE Wireless and Microwave Strategy Conference (WAMICON), **(2006)**.
[10] D. Dardari, A. Conti, U. Ferner, A. Giorgetti and M. Z. Win, "Ranging with ultra-wide bandwidth signals in multipath environments", Proceedings of the IEEE, vol. 97, no. 2, (**2009)**, pp. 404-426.
[11] Y. Zhang, A. K. Brown, W. Q. Malik and D. J. Edwards, "High resolution 3D angle of arrival determination for indoor UWB multipath propagation", IEEE Transactions on Wireless Communications, vol. 7, no. 8, (**2010)**, pp. 3047-3055.
[12] D. Dardari, A. Giorgetti and M.Z. Win. " Time of arrival estimation of UWB signals in the presence of narrowband and wideband interference", IEEE International Conference on Ultra-Wideband (ICUWB), **(2007)**.
[13] M. Bocquet, C. Loyez and A. BenlarbiDelai, " Using enhanced TDOA measurement for indoor localization", IEEE Microwave and WireleSG Components Letters, vol. 15, no.10, (**2005)**, pp. 612-614.

[14] A. Abbasi and M.H. Kahaei, "Improving source localization in LOS and NLOS multipath environments for UWB signals". International CSI Computer Conference (CSICC), **(2009)**.
[15] I. Guvenc and Z. Sahinoglu, "Multi-scale energy products for TOA estimation in IRUWB systems", IEEE Global Telecommunications Conference, (GLOBECOM), **(2005)**.
[16] A. Y. Z. Xu, E. K. S. Au, A. K.S. Wong and Q. Wang, "A novel threshold based coherent TOA estimation for IR-UWB systems", IEEE Transactions on Vehicular Strategy, vol. 58, no. 8, **(2009)**, pp. 4675-4681.
[17] I. Guvenc and Z. Sahinoglu, "Threshold selection for UWB TOA estimation based on Skewness analysis", IEEE Communications Letters, vol. 9, no. 12, **(2005)**, pp. 1025-1027.
[18] I. Guvenc and Z. Sahinoglu. "Threshold based TOA estimation for impulse radio UWB systems", IEEE International Conference on Ultra-Wideband, **(2005)**.
[19] IEEE Standard for Information strategy--Local and metropolitan area networks--Specific requirements--Part 15.3: Wireless Medium Access Control (MAC) and Physical Layer (PHY) Specifications for High Rate Wireless Personal Area Networks (WPAN) amendment 2: millimeter-wave-based alternative physical layer extension". IEEE Computer Society, IEEE 802.15.06-0474-00-003c. New York, USA, **(2009)**
[20] "802.11n-2009-IEEE Standard for Information strategy-- Local and metropolitan area networks--Specific requirements--Part 11: Wireless LAN Medium Access Control (MAC)and Physical Layer (PHY) Specifications Amendment 5: Enhancements for Higher Throughput", IEEE Computer Society, IEEE 978-0-7381-6731-2. New York, USA, **(2009)**.
[21] C. R. Andersonn and T. S. Rappaport, "In-building wideband partition loss measurements at 2.5 and 60GHz", IEEE Transactions on Wireless Communications, vol. 3, no. 3, **(2004)**, pp. 922-928.
[22] S. Collong, G. Zaharia and G. E. Zein, "Influence of the human activity on wide-band characteristics of the 60GHz indoor radio channel", IEEE Transactions on Wireless Communications, vol. 3, no. 6, **(2005)**, pp. 2396-2406
[23] A. Maltsev, R. Maslennikov and A. Sevastyanov, "Experimental investigations of 60GHz WLAN systems in office environment", IEEE Journal on Selected Areas in Communications, vol. 27, no. 8, **(2009)**, pp. 1488-1499.
[24] M. G. Sanchez, A. V. Alejos and I. Cuinas, "Comparision of space diversity performance in indoor radio channels at 40GHz and 60GHz", Proc. of European Conference on Wireless Strategy, Amsterdam, **(2008).**
[25] H. B. Yang, "Channel characteristics and transmission performance for various channel configurations at 60GHz", EURASIP Journal on Wireless Communications and Networking, vol. 2007, no. 1, **(2007)**, pp. 43-43.
[26] N. Li, "Study on the properties of 60 GHz impulse radio communication system", Qingdao: Ocean University of China, **(2012)**.
[27] X. Cui, C. Wu and J. Li, "UWB simulation of energy detection algorithm based on the Internet of things", Application of micro-computer, vol, 27, no. 9, **(2011)**, pp.20-26.

Authors

Xiaolin Liang now studies in College of Information Science and Engineering and is a master candidate in Ocean University of China. His research interests include ultra-wideband radio systems, 60GHz wireless communication system.

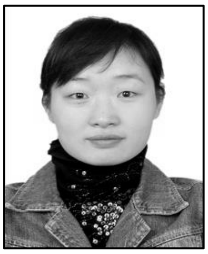

Tingting Lu received the Ph. D. degree in College of Information Science and Engineering from Ocean University of China in 2013. She is now a lecture in College of Information Science and Engineering. Her research interests include ultra-wideband radio systems, 60GHz wireless communication system.

Hao Zhang received the MBA degree in New York Institute of

Technology, American in 2001 and the Ph. D. degree in Electrical and Computer Engineering from the University of Victoria, Canada in 2004. He was a Project Manager for Microsoft Inc. in United States during January 2000-May 2000. During 2004-2008, he was the Vice President for the United States Gamma Capital Inc. He is now an Adjunct Assistant Professor in the Department of Electrical and Computer Engineering. Also he becomes a professor and the Ph. D. supervisor in College of Information Science and Engineering from Ocean University of China in 2006. His research concerns ultra-wideband radio systems, 60GHz wireless communication system and MIMO wireless communication.

T. Aaron. Gulliver received the Ph. D. degree in Electrical and Computer Engineering from the University of Victoria, Canada in 1989. He is now a professor and the Ph. D. supervisor in the Department of Electrical and Computer Engineering. In 2002, he becomes a Fellow of the Engineering Institute of Canada, and in 2012 a Fellow of the Canadian Academy of Engineering. He is also a senior member of IEEE. His research concerns information theory and communication theory, algebraic coding theory and smart grid and ultra-wideband communication.